Microelectronic Engineering 88 (2011) 2345–2348

Contents lists available at ScienceDirect

Microelectronic Engineering

journal homepage: www.elsevier.com/locate/mee

# Influence of silicon orientation and cantilever undercut on the determination of the Young's modulus of thin films

H. Nazeer [a,*], L.A. Woldering [a], L. Abelmann [a], M.D. Nguyen [a], G. Rijnders [a], M.C. Elwenspoek [a,b]

[a] MESA+, Institute for Nanotechnology, University of Twente, P.O. Box 217, 7500 AE, Enschede, The Netherlands
[b] FRIAS, Albert-Ludwigs University, Albertst. 19, 79104 Freiburg, Germany

ARTICLE INFO

*Article history:*
Available online 19 January 2011

*Keywords:*
Young's modulus
PZT
Resonance frequency
Orientation
Cantilever
DRIE
Finite-element method

ABSTRACT

The Young's modulus of thin films can be determined by deposition on a micronsized Si cantilever and measuring the resonance frequency before and after deposition. The accuracy of the method depends strongly on the initial determination of the mechanical properties and dimensions of the cantilever. We discuss the orientation of the cantilever with respect to the Si crystal, and the inevitable undercut of the cantilever caused by process inaccuracies. By finite element modelling we show that the Young's modulus should be used instead of the analytical plate modulus approximation for the effective Young's modulus of Si cantilevers used in this work for both the ⟨1 0 0⟩ and ⟨1 1 0⟩ crystal orientation. Cantilever undercut can be corrected by variation of the cantilever length. As an example, the Young's modulus of $PbZr_{0.52}Ti_{0.48}O_3$ (PZT) thin films deposited by pulsed laser deposition (PLD) was determined to be 99 GPa, with 1.4 GPa standard error.

© 2011 Elsevier B.V. All rights reserved.

## 1. Introduction

Design of micro electromechanical systems (MEMS) requires detailed information about material parameters such as the Young's modulus. As industry is increasingly focusing on micro devices, we need information on the mechanical properties of materials in the thin film domain. These properties can differ from those of bulk materials [1]. Many micro sized structures such as cantilevers, membranes and bridges have been employed as test structures for determining the mechanical properties of thin films. Cantilevers are among the most widely used test structures for this purpose [2,3].

Calculation of the resonance frequency of cantilevers fabricated from silicon, which is an elastically anisotropic material, requires the use of an appropriate effective Young's modulus [4]. A technique is introduced to determine the appropriate effective Young's modulus that needs to be used in the resonance frequency calculation of our cantilevers. We took extra care to eliminate the errors in the determination of the effective Young's modulus of the thin films deposited on the cantilevers. At this precision, conventional analytical expressions [5] to calculate resonance frequencies of silicon cantilevers need to be verified. We used 3D finite-element (FE) simulations to estimate the deviations between these simulations that use anisotropic elastic properties of silicon and the values calculated analytically for our ⟨1 1 0⟩ and ⟨1 0 0⟩ aligned cantilevers.

Any uncertainty about the length of cantilevers introduces an error in the resonance frequency calculations of silicon cantilevers as well as in the determined value of effective Young's modulus of thin film. In order to be precise, we determined the effective undercut length using least square fitting of the measured resonance frequencies data for cantilevers with a wide range of lengths. The obtained effective length of the cantilevers is then used in the calculations of the effective Young's modulus of the thin film.

## 2. Theory

The resonance frequency of a cantilever is calculated by using the analytical relation defined in Eq. (1) [5]:

$$f_n = \frac{C^2 t_s}{2\pi L^2}\sqrt{\frac{E_s^*}{12\rho}} \tag{1}$$

here $f_n$ is the resonance frequency, $C$ is a constant which depends on the vibration mode, $C = 1.875$ for fundamental resonance frequency $(f_0)$, $E_s^*$ is the effective Young's modulus of silicon, $\rho$ is the density of silicon [6], $t_s$ is the thickness and $L$ is the length of the cantilevers. Eq. (1) is a two dimensional approximation. The third dimension is taken into account in the effective Young's modulus, which depends on the width of the cantilever. If the width is much larger than the length, the strain along that direction is zero. In this case, for very thin cantilevers and isotropic materials we can use the plate modulus $E/(1-\nu^2)$ as an approximation for the effective Young's modulus $E^*$ [7], where $E$ and $\nu$ are the Young's modulus

* Corresponding author.
*E-mail address:* h.nazeer@utwente.nl (H. Nazeer).

0167-9317/$ - see front matter © 2011 Elsevier B.V. All rights reserved.
doi:10.1016/j.mee.2011.01.028

**Table 1**
Elastic anisotropic properties of single crystal silicon. Values of $E$ and $v$ are taken from [8].

| Direction | $E$ (GPa) | $v$ | $E/(1-v^2)$ (GPa) |
|---|---|---|---|
| *Crystal plane {100}* | | | |
| ⟨110⟩ | 168.9 | 0.064 | 169.8 |
| ⟨100⟩ | 130.2 | 0.279 | 141.0 |

**Table 2**
Calculated and simulated fundamental resonance frequency of silicon cantilevers with length $L = 300$ μm, thickness $t_s = 3$ μm and width $w = 30$ μm.

| Direction | Calculated $f_0$ (Hz) using $E$ | Calculated $f_0$ (Hz) using $E/(1-v^2)$ | FE-simulations (Hz) |
|---|---|---|---|
| ⟨110⟩ | 45,834 | 45,956 | 45,978 |
| ⟨100⟩ | 40,242 | 41,878 | 40,541 |

and Poisson's ratio, see Table 1. With reducing width, the stress in that direction is relaxed and the effective Young's modulus decreases to $E$ for a width much smaller than the cantilever length. In our situation, the cantilever width is smaller than the length. Moreover, single crystal silicon is anisotropic [8], so the two-dimensional situation was checked by finite element calculations for silicon cantilevers aligned parallel to the ⟨110⟩ and ⟨100⟩ crystal directions of the silicon crystal lattice.

Full 3D finite-element simulations were carried out using the COMSOL software package and compared with the analytical results that were obtained using Eq. (1). To define cantilevers parallel to the ⟨110⟩ orientation in COMSOL, the cantilever geometry was drawn in the xy-plane with the length axis parallel to the $x$-axis and then rotated 45° around the $z$-axis. For the ⟨100⟩ cantilevers, no rotation was given to the cantilever. Standard anisotropic elastic properties of single crystal silicon, as defined in the material section of the COMSOL, were used for the simulations. The elastic stiffness coefficients are identical to values quoted in the literature [8].

Table 2 lists the analytical calculations of resonance frequencies using Eq. (1) and the results of the FEM simulations of a silicon cantilever with a length of 300 μm, thickness of 3 μm and width of 30 μm. The analytical values of the resonance frequencies calculated using Young's modulus $E$ agree with the FEM simulations to within 0.3% for the ⟨110⟩ direction and 0.7% for ⟨100⟩ direction. The FEM results differ by 3% when using the plate modulus $E/(1-v^2)$ for ⟨100⟩ aligned cantilevers. The results verify that, for the cantilever geometry which we have used in this work, the factor of $(1-v^2)$ cannot be used in the denominator of $E$.

## 3. Fabrication

To ensure precise control of the dimensions of the cantilevers, we fabricated our 3 μm thick silicon cantilevers in a dedicated SOI/MEMS fabrication process. The cantilevers are designed such that their length varies from 250 μm to 350 μm in steps of 10 μm with a fixed width of 30 μm. Cantilevers were defined by standard lithography and an-isotropically etched by deep reactive ion etching (DRIE) [9] on the front side of (100) single crystal silicon on insulator (SOI) wafers. In the last step of the front side processing, 4 μm thick polyimide pyralin was spin-coated on the front side, see Fig. 1a. In particular, this layer protects the cantilevers from any damage during the back side processing of the wafers [10].

Subsequently, cantilevers were released from the handle wafer by making through holes from the backside of the wafers using DRIE, see Fig. 1b. Finally, the cantilevers were released by etching of the buried oxide layer using vapours of hydrofluoric acid (VHF) [11], see Fig. 1c. To measure resonance frequencies of the cantilevers in the ⟨110⟩ and ⟨100⟩ crystal directions of silicon, cantilevers were fabricated aligned parallel to the ⟨110⟩ and ⟨100⟩ crystal direction of the silicon crystal lattice, see Fig. 2. The fabricated cantilevers were characterised and inspected by scanning electron and optical microscopy.

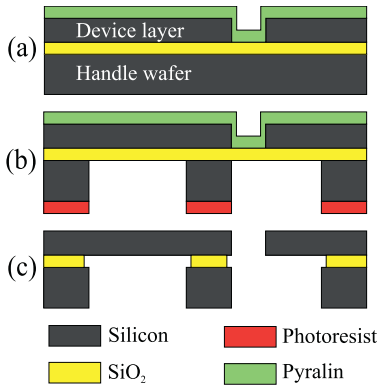


**Fig. 1.** Outline of the fabrication process to obtain cantilevers on the front side of the wafers. (a) DRIE of the silicon device layer and application of polyimide pyralin as protective layer, (b) wafer through DRIE, (c) isotropic etching of the buried oxide layer using VHF. Dimensions are not on scale.

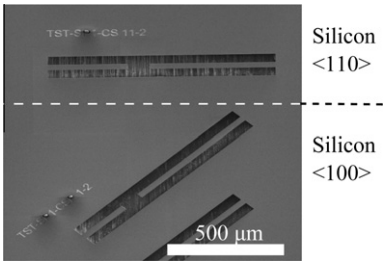


**Fig. 2.** Scanning electron micrograph of the fabricated cantilevers. Cantilevers with a range of lengths are aligned parallel to the ⟨110⟩ and ⟨100⟩ crystal orientations of the silicon wafer. Each slot contains two cantilevers with different lengths. In this way the available space on the chips is most efficiently used and process variation is reduced.

## 4. Measurements

The resonance frequency of the cantilevers was measured under ambient conditions by using a MSA-400 micro system analyser scanning laser-Doppler vibrometer. The measured resonance fre-

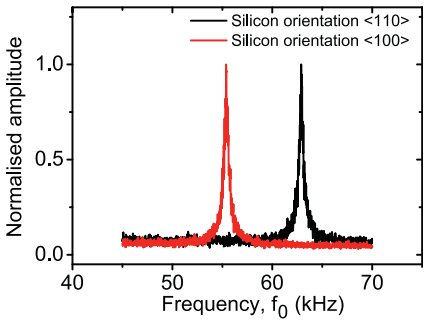


**Fig. 3.** The difference in resonance frequency of identical cantilevers, aligned in the ⟨110⟩ and ⟨100⟩ crystal directions of the silicon crystal lattice. The amplitude is normalised to the maximum value.

quencies for cantilevers of length around 250 μm, width around 30 μm, and thickness around 3 μm are shown in Fig. 3. The identical cantilevers are aligned parallel to the ⟨110⟩ and ⟨100⟩ crystal orientations of silicon. The difference in the fundamental resonance frequency for two differently oriented identical cantilevers can be seen clearly from Fig. 3. This difference is solely caused by the different effective Young's modulus for the two crystal directions.

From Eq. (1) we observed that the most critical dimensional parameters are thickness and length. Ideally, the fabricated cantilever should follow the geometrical dimensions as designed on mask, see Fig. 4a. Unfortunately, the DRIE process used for the release of cantilevers from the handle wafer introduces an undercut in the cantilevers. This undercut, shown in Fig. 4b, is caused by over-etching and increases the length of cantilevers.

Since undercut cannot be avoided in this fabrication process, it must be included in the resonance frequency calculations using Eq. (1). The effect of undercut is included by adding an effective undercut length $\Delta L'$ to the length $L$ of cantilevers [12,13]. The effective length $L + \Delta L'$ of cantilevers is determined by least square fitting of the measured resonance frequencies data for fabricated cantilevers with a range of length, see Fig. 5. Eq. (1) is used as a fitting function after replacing $L$ with $L + \Delta L'$ and keeping $\Delta L'$ as a free parameter in the fitting routine. The ratio of the measured resonance frequencies to their respective thickness are shown in Fig. 5 for a range of cantilevers aligned parallel to the ⟨110⟩ and ⟨100⟩ crystal directions of silicon. The fitting curves are shown by solid lines in the Fig. 5 where as squares and circles represents the measured data for ⟨110⟩ and ⟨100⟩ cantilevers, respectively. The effective undercut length $\Delta L'$ determined from the fitting routine was found to be 5 μm for the ⟨110⟩ crystal direction and 1 μm for the ⟨100⟩ crystal direction of silicon. The coefficients of determination were both 0.99.

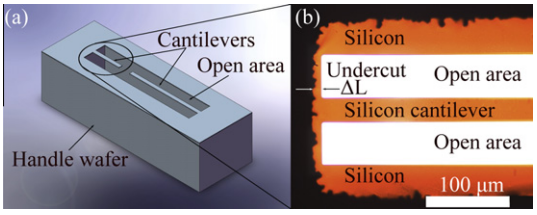


**Fig. 4.** The undesired undercut in the cantilevers was created by the back side etching of the handle wafer. (a) Pictorial representation of the ideal released cantilevers without undercut. (b) Optical micrograph of the ⟨110⟩ cantilever showing undercut. Rough sides of the undercut can be clearly seen.

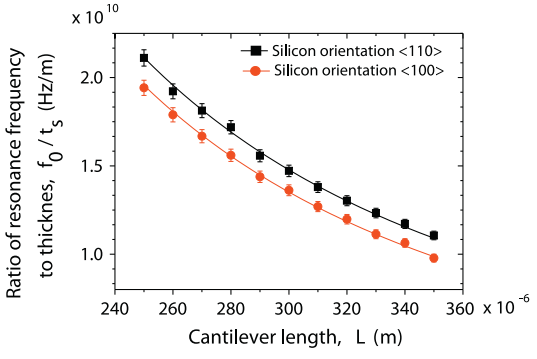


**Fig. 5.** Least square fitting of the fundamental resonance frequency of cantilevers. Ratio of the resonance frequency to their respective thickness was plotted against length. The effective undercut length $\Delta L'$ was obtained by fitting the resonance frequency data points using least square method as shown by the solid lines. Squares are measured values for the ⟨110⟩ cantilevers and circles represents ⟨100⟩ aligned cantilevers.

## 5. Results and discussion

The experimentally measured resonance frequencies for the range of cantilevers length agrees with the FE simulations and the analytically calculated values when using Young's modulus as the appropriate effective Young's modulus. We found a 3% variation between the FE simulations results and analytically calculated values of the resonance frequency in the ⟨100⟩ crystal direction of silicon when using plate modulus approximation. Without a factor of $(1 - \nu^2)$ in the denominator, the variation is only 0.7%. Therefore the plate modulus approximation is not valid for the cantilevers used in this work. This is in agreement with the analysis by McFarland, who suggests use of the Searle parameter to differentiate between beams and plates [14].

As an example of the determination the Young's modulus of the thin films, we deposited 100 nm thick PZT by PLD on these cantilevers. The Young's modulus of the PZT thin film is calculated by using the measured change in resonance frequency before and after the epitaxial deposition. The Young's modulus of PZT thin film was found to be 99 GPa. The value of the Young's modulus of the PZT thin film deposited by PLD is in the same order as values quoted in the literature for sol–gel [15] and sputter deposited [16] PZT. Details of the Young's modulus measurement of the PZT thin films is beyond the scope of this paper and will be published elsewhere.

## 6. Conclusions

We demonstrated a method to determine the best approximation for the effective Young's modulus of cantilevers. This method is generally applicable for arbitrary cantilever dimensions. Furthermore, we determined that the analytical relation for resonance frequency calculations using $E^* = E$ for silicon cantilevers is very precise in both the ⟨110⟩ and ⟨100⟩ directions. When using plate modulus approximation for the ⟨100⟩ direction, the deviation of the analytical values compared to the FE simulations is 3%. As an example we utilised these cantilevers to determine the Young's modulus of the epitaxially grown PZT thin film deposited by PLD. The Young's modulus of PZT is found to be 99 GPa with a standard error of 1.4 GPa.

## Acknowledgements

The authors gratefully acknowledge the support of the Netherlands SmartMix Program (SmartPie), M.J. de Boer for etching, R.G.P. Sanders for laser Doppler vibrometer measurements, J.G.M. Sanderink for assistance with SEM, and N. Tas for helpful discussions.

## References

[1] P. Delobelle, O. Guillon, E. Fribourg-Blanc, C. Soyer, E. Cattan, D. Rèmiens, Appl. Phys. Lett. 85 (2004) 5185–5187.
[2] M.D. Nguyen, H. Nazeer, K. Karakaya, S.V. Pham, R. Steenwelle, M. Dekkers, L. Abelmann, D.H.A. Blank, G. Rijnders, J. Micromech. Microeng. 20 (2010) 085022.
[3] E. Finot, A. Passian, T. Thundat, Sensors 8 (2008) 3497–3541.
[4] S. Kaldor, I. Noyan, Appl. Phys. Lett. 80 (2002) 2284–2286.
[5] E. Volterra, E.C. Zachmanoglou, Dynamics of Vibrations, CE Merrill Books, 1965.
[6] R.D. Deslattes, A. Henins, H.A. Bowman, R.M. Schoonover, C.L. Carroll, I.L. Barnes, L.A. Machlan, L.J. Moore, W.R. Shields, Phys. Rev. Lett. 33 (1974) 463–466.
[7] P.A. Rasmussen, Cantilever-based Sensors for Surface Stress Measurements, Ph.D. Thesis, Technical.
[8] W.A. Brantley, J. Appl. Phys. 44 (1973) 534–535.
[9] H.V. Jansen, M.J. De Boer, S. Unnikrishnan, M.C. Louwerse, M.C. Elwenspoek, J. Micromech. Microeng. 19 (2009) 033001.

[10] N.C. Loh, M.A. Schmidt, S.R. Manalis, J. Microelectromech. Syst. 11 (2002) 182–187.
[11] J. Anguita, F. Briones, Sens. Actuators A 64 (1998) 247–251.
[12] K. Babaei Gavan, E.W.J.M. van der Drift, W.J. Venstra, M.R. Zuiddam, H.S.J. van der Zant, J. Micromech. Microeng. 19 (2009) 035003.
[13] A.N. Cleland, M. Pophristic, I. Ferguson, Appl. Phys. Lett. 79 (2001) 2070–2072.
[14] A. McFarland, M. Poggi, L. Bottomley, J. Colton, J. Micromech. Microeng. 15 (2005) 785–791.
[15] B. Piekarski, D. DeVoe, M. Dubey, R. Kaul, J. Conrad, Sens. Actuators A 91 (2001) 313–320.
[16] T.-H. Fang, S.-R. Jian, D.-S. Chuu, J. Phys.: Condens. Matter. 15 (2003) 5253–5259.